Journal of Electrical Engineering, Electronics, Control and Computer Science – JEEECCS, Volume 7, Issue 24, pages 39-46, 2021

Fixed Wing Unmanned Aerial Vehicle Control by Using a Non-linear PID Controller

[1]Selamawit Mekuria, [2]Mebaye Belete, [3]Betelehem Niguse
Addis Ababa Science and Technology University
Addis Ababa, Ethiopia
[1]selamawit.mekuria4@gmail.com, [2]mebaye.belete@aastu.edu.et, [3]bettyniguse15@gmail.com

Abstract – **This paper presents the modeling and control of a fixed-wing unmanned aircraft. The flight dynamics of this system is obtained by using Newton's second law of motion. After that, a non-linear PID (NPID) controller is designed for this system which is also useful to minimize the difference that could be caused when using a linearized model of this system. To check the robustness of the controllers, an external disturbance is added throughout the simulation time; in addition, the controller gain values are kept in an acceptable range. Furthermore, H_2 and H_∞ norms have been used to get a numerical representation of the robustness; the frequency of the control signal to the system has been measured. Finally, using the non-linear model of the system; the designed controller is simulated on MATLAB Simulink software. The results show that the states followed the desired trajectory with an acceptable control effort in the presence of external disturbance having an input signal that would not be harmful to equipment.**

Keywords: UAV, fixed-wing UAV, Flight Dynamics, PID, NPID

I. INTRODUCTION

UAV is a short abbreviation for unmanned aerial vehicles. These vehicles have many applications. They can be used in missions that are dangerous to humans or even tiresome. Even though they can be classified under different categories, they mainly fall under fixed-wings and rotary-wing UAVs. Fixed-wing UAVs have the capability of long-range flight due to the structure they possess; this structure also gives them the ability to carry greater payload and still fly at high speed. Conversely, it is still a challenge to control these aircrafts to the fullest because of modeling uncertainties and external disturbances. Different control algorithms have been formulated to enhance or rather tackle any flight problems that a fixed-wing UAV might face. To mention some from both linear and non-linear control methods; PID [1], adaptive PID [2], optimal control [3] are common. Extended observers have also been used together with different controllers like SMC to overcome problems that arise from external disturbances [4].

Chosen for its simplicity and less computational resources a PID controller remains to be in the market for the control of a UAV [5] [6]. Nonetheless, to design a PID controller linearization of the system dynamics is the first step. In [7], a fixed-wing aircraft is linearized to evaluate the difference and similarity between the linear and non-linear version of the model; from the simulation analysis, it showed that there are differences in frequency and amplitude between the two approaches; and this amplitude difference keeps on growing when deflection of the control surfaces increases, this will, in turn, lead to modeling uncertainty. Keeping in mind that this classical controller is still in use. In this paper, a non-linear PID controller is designed to minimize the difference that could be caused when using a linear model.

To check the robustness and performance of the controller, an external disturbance is added and all the controller gains are taken in an acceptable range. The organization of this paper is presented as follows; section 2 presents the mathematical modeling of a fixed-wing UAV. Followed by the controller design in section 3. Simulation and result analysis are elaborated in section 4. Lastly, the conclusion and recommendation are found in section 5.

II. MATHEMATICAL MODELLING

To simplify the modeling, the following assumptions are taken. The aircraft is assumed to be a rigid body in space and the mass of the UAV is constant. Furthermore, the earth is assumed to be an inertial frame of reference, the aircraft is symmetric on the XZ plane, and the CG of the aircraft body coincides with the body-fixed frame.

Coordinate systems are used to locate a certain point in space; in this case, we use it to describe the forces acting on the aircraft and the motion that comes afterward. In this regard, the coordinate systems can be given as in [8]. The inertial frame (fixed frames that are fixed to the distant stars and do not rotate with earth), body carried frame (frames that are attached to the aircraft and moves with the aircraft but do not rotate), body-fixed reference frame (attached to the center of gravity of the aircraft and rotates with the aircraft) and wind reference frame (used to express the forces and moments acting on the unmanned aircraft due to wind). The direct cosine matrices R_e^b is taken to rotate from earth frame to body frame. (See [8]).

$$R_e^b = \begin{bmatrix} c_\psi c_\theta & s_\psi c_\theta & -s_\theta \\ -s_\psi c_\phi + s_\theta c_\psi s_\phi & s_\phi s_\psi s_\theta + c_\phi c_\psi & s_\phi c_\theta \\ s_\phi s_\psi + c_\phi s_\theta c_\psi & c_\phi s_\theta s_\psi - c_\psi s_\phi & c_\phi c_\theta \end{bmatrix} \quad (1)$$

The kinematics and dynamics of the fixed-wing UAV are analyzed by using the Newton-Euler method as in [9].

$$F_b = m(\dot{v}_b^g + \dot{\omega} \times r_b^{*cg} + \omega \times v_b^g + \omega \times [\omega \times r_b^{*cg}]) \quad (2)$$

$$\sum_{i=1}^{N} r_b^i \times \frac{d}{dt}(m_i v_u^i) = \sum_{i=1}^{N} m_i r_b^i \times \left(\frac{\partial v_b^g}{\partial t} + \omega \times v_b^g\right) + \sum_{i=1}^{N} m_i r_b^i \times \left[\frac{\partial \omega}{\partial t} \times r_b^i\right] + \sum_{i=1}^{N} m_i r_b^i \times [\omega \times [\omega \times r_b^i]] \quad (3)$$

Where $F_b = [x, y, z]^T$ are the external forces defined in the body frame. $r_b^{*cg} = [x_{cg}, y_{cg}, z_{cg}]$: are the locations of CG on the body frame. $v_b^g = [u, v, w]^T$: are body frame expressions of earth linear velocity components. $\omega = [p, q, r]^T$: are body frame expressions of earth angular velocity components.

Using equations (2) and (3), the generalized 6-DOF equation that describes the motion including the time rate of change of Euler angles can be summarized.

$$\left.\begin{aligned} \dot{u} &= -wq + vr + \frac{1}{m}(x) \\ \dot{v} &= -ru + wp + \frac{1}{m}(y) \\ \dot{w} &= -vp + uq + \frac{1}{m}(z) \\ L &= pq + \dot{p} I_{xx} + I_{xz}\dot{r} + rq(I_{zz} - I_{yy}) \\ M &= prI_{zz} + prI_{xx} + \dot{q} I_{yy} + r^2 I_{xz} - p^2 I_{xz} \\ N &= I_{zx}\dot{p} + (I_{yy} - I_{xx}) pq + \dot{r} I_{zz} - rqI_{zx} \end{aligned}\right\} \quad (4)$$

$$\begin{bmatrix} \dot{\phi} \\ \dot{\theta} \\ \dot{\psi} \end{bmatrix} = \begin{bmatrix} t_\theta q s_\phi + p + t_\theta r c_\phi \\ c_\phi q - s_\phi r \\ s_\phi \dfrac{q}{c_\theta} + c_\phi \dfrac{r}{c_\theta} \end{bmatrix} \quad (5)$$

To avoid singularity or gimbal lock, the Euler angle boundaries are taken as:

$$-\frac{\pi}{2} < \phi < \frac{\pi}{2}, -\frac{\pi}{2} < \theta < \frac{\pi}{2}, -\pi < \psi < \pi$$

A. Forces and Moments

The main moments and forces acting on a fixed-wing aircraft are

I. Gravitational force $F_b^g = [mg, 0, 0]^T$,

II. Thrust force $F_{tr} = [F_{tr}, 0, 0]^T$,

III. Thrust moment $M_{tr} = [M_{tr}, 0, 0]^T$,

IV. Aerodynamic-forces

$$[F_L, F_D, F_Y] = \frac{1}{2}\rho v_a^2 s R_w^b [C_L, C_D, C_Y]^T \text{, and}$$

V. Aerodynamic-moment

$$[M_L, M_D, M_Y] = \frac{1}{2}\rho v_a^2 s R_w^b [bC_l, cC_m, bC_n]^T$$

$$R_w^b = \begin{bmatrix} c\beta c\alpha & -c\alpha s\beta & -s\alpha \\ s\beta & c\beta & 0 \\ s\alpha c\beta & -s\beta s\alpha & c\alpha \end{bmatrix}$$

Where R_w^b the rotational matrices from wind frame to body frame is, $v_a = \sqrt{u^2 + v^2 + w^2}$ is the airspeed, $\alpha = \tan^{-1}\left(\frac{w}{u}\right)$ is the angle of attack, and $\beta = \sin^{-1}\left(\frac{v}{v_a}\right)$ is the sideslip. Furthermore, wingspan *b*, chord *c*, and surface area of the wing *s* are constants. Mass is denoted by *m*, gravity is denoted by *g* and ρ denotes the air density. C_L and its corresponding arguments are the non-dimensional coefficients and are presented in equation (6).

$$\left.\begin{aligned}
C_D &= c_{Do} + c_D^{\alpha}\alpha + c_D^{q}\frac{c}{2v_a}q + c_D^{\delta e}\delta_e \\
C_L &= c_{L0} + c_L^{\alpha}\alpha + c_L^{q}\frac{c}{2v_a}q + c_L^{\delta e}\delta_e \\
C_Y &= c_{yo} + c_y^{\beta}\beta + c_y^{p}\frac{b}{2v_a}p + c_y^{r}\frac{b}{2v_a}r + c_y^{\delta r}\delta_r + c_y^{\delta a}\delta_a \\
C_l &= c_{lo} + c_l^{\beta}\beta + c_l^{p}\frac{b}{2v_a}p + c_l^{r}\frac{b}{2v_a}r + c_l^{\delta r}\delta_r + c_l^{\delta a}\delta a \\
C_M &= c_{mo} + c_m^{\alpha}\alpha + c_m^{q}\frac{c}{2v_a}q + c_m^{\delta e}\delta_e \\
C_n &= c_{no} + \beta c_n^{\beta} + \frac{b}{2v_a}pc_n^{p} + \frac{b}{2v_a}rc_n^{r} + \delta_r c_n^{\delta r} + \delta a c_n^{\delta a}
\end{aligned}\right\} \tag{6}$$

δ_a , δ_e and δ_r are the control surfaces of the aircraft. Together with thrust force, they are the four inputs of this system.

III. CONTROLLER DESIGN

The conventional PID is one type of classical controller design technique that is widely used in industrial control systems. This controller is a closed-loop

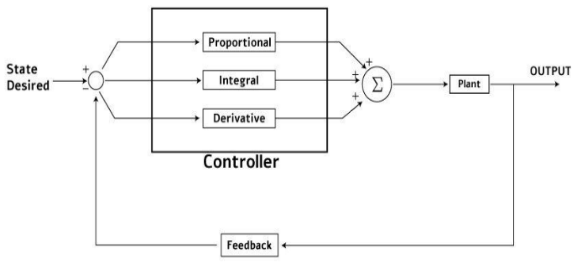

Figure 1. Linear PID

From Figure 1 we can see it consists of a plant to be controlled, feedback that measures the output, and a controller. The controller can be given mathematically as:

$$U = k_p\left(e + \frac{1}{\tau_i}\int_{\tau_0}^{\tau} edt + \frac{1}{\tau_d}e\right)$$

$$U = k_p e + k_i\int_{\tau_0}^{\tau} edt + k_d e \tag{7}$$

Where U is the control input k_p, k_i, k_d are the proportional, integral, and derivative gains respectively. The proportional gain is used to reduce the error. The integral gain is used to reduce steady-state error. Whereas the derivative gain is for damping

In this paper, the non-linear version of this classical controller is designed simply because a linear controller cannot be implemented for a non-linear system. NPID controller is used in achieving things like reduced rise time for step inputs, better tracking accuracy, and increased damping [10]. The algorithm of this controller is based on a non-linear function as an essential part. Hence the NPID controller is given us:

$$\begin{aligned} u = {} & k_p\psi(e_p,\alpha_p,\delta_p) + k_i\psi(e_i,\alpha_i,\delta_i) + \\ & k_d\psi(e_d,\alpha_d,\delta_d) \end{aligned} \tag{8}$$

Where k_p, k_i, k_d are the controller gains and they are the same as the ones found in classical control. α is the error weighting. δ is a parameter that defines the linear area. $\psi(x,\alpha,\delta)$ is the non-linear function defined by

$$\psi(x,\alpha,\delta) = \begin{cases} |x|^{\alpha}.sign(x), & \text{when } |x| > \delta \\ \delta^{\alpha-1}.x, & \text{when } |x| \le \delta \end{cases} \tag{9}$$

From [10], α_p should be larger than one to get a more sensitivity to small errors, α_i should be between the values of -1 and 0 to reduce the integral action when the error is large and lastly the error weighing of the derivative, α_d , should be larger than one to make the differential gain smaller at a smaller error. δ Defines the linear area in the non-linear function and since the aircraft's system is highly non-linear δ is chosen to have a small value. Hence, for the reasons mentioned, $[\alpha_p, \alpha_i, \alpha_d]$ is chosen as $[1.6, -0.5, 1.1]$ and δ as 0.01.

Since there is no tuning mechanism to tune the gain values, first $\psi(x,\alpha,\delta)$ is found by different methods like gradient descent, the hessian matrix, extreme value theorem and mean value theorem for both attitude and airspeed control. The gradient descent method is used to find only the relative or absolute minima and the Hessian matrix is used to find the maxima and minima for a function of several variables. In this paper, the mean value theorem is used to find the error $\psi(x,\alpha,\delta)$.

Theorem 2 [11]: "if f is a continuous function over the closed, bounded interval [a, b], then there is a point in [a, b] at which f has a relative maximum over [a, b] and there is a point in [a, b] at which f has a relative minimum over [a, b]". Rewriting equation (9) as:

$$\psi(x,\alpha,\delta) = \begin{cases} |x|^{\alpha}, & \text{when } x > \delta \\ -|x|^{\alpha}, & \text{when } x < \delta \\ \delta^{\alpha-1}.x, & \text{when } -\delta \le |x| \le \delta \end{cases} \tag{10}$$

For attitude and airspeed control, first, assume the initial control signal as 0.3 rad and 18N respectively. Furthermore, say these values are produced equally by the proportional, integral, and derivative. For airspeed:

$$k_p\psi(e_p,\alpha_p,\delta_p) + k_i\psi(e_i,\alpha_i,\delta_i) + k_d\psi(e_d,\alpha_d,\delta_d) = 18N$$

For attitude

$$k_p\psi(e_p,\alpha_p,\delta_p) + k_i\psi(e_i,\alpha_i,\delta_i) + k_d\psi(e_d,\alpha_d,\delta_d) = 0.3rad$$

Hence:

$$k_p\psi(e_p,\alpha_p,\delta_p)=6N$$
$$k_i\psi(e_i,\alpha_i,\delta_i)=6N$$
$$k_d\psi(e_d,\alpha_d,\delta_d)=6N$$
$$k_p\psi(e_p,\alpha_p,\delta_p)=0.1rad$$
$$k_i\psi(e_i,\alpha_i,\delta_i)=0.1rad$$
$$k_d\psi(e_d,\alpha_d,\delta_d)=0.1rad$$

Assuming an initial error boundary of [-0.007, 0.0001] for attitude and [-0.03, 1.5] for airspeed, the gain value is found as follows.

Step 1: Find the derivative of the function $\psi(x,\alpha,\delta)$.

Step 2: find the critical point at $\psi'(x,\alpha,\delta)=0$.

Step 3: solve for $\psi(x,\alpha,\delta)$ at critical point and boundary conditions.

Step 4: Repeat the process for all three $\psi(x,\alpha,\delta)$ functions and the maximum value is the relative maxima and the minimum value is the relative minima. Computing the gain values for the error values obtained at step four gives:

$$\left.\begin{aligned} k_p &= [333.3, 251256] \\ k_i &= [0.0001, 0.00082] \\ k_d &= [29.4, 2500] \end{aligned}\right\} \text{For attitude}$$

$$\left.\begin{aligned} k_p &= [1.05, 540] \\ k_i &= [0.347, 2.44] \\ k_d &= [1.28, 100] \end{aligned}\right\} \text{For airspeed}$$

Hence, the attitude and airspeed gains are presented as [334, 0.001, 34.6] and [150, 0.39, 1.3] respectively.

A. Design Of NPID Algorithm

In this section, a non-linear PID is designed for attitude and airspeed control of the aircraft. Using Hurwitz's characteristics equation to create the sliding manifold as in [12].

$(a_1+a_2s+\dots+a_ms^{m-1})=0$ …Hurwitz characteristics

1) Design of NPID Controller for Attitude Tracking Problem

Referring back to equation (3); we will drive expression for attitude control.

$$\sum_{i=1}^{N} m_i r_b^i \times\left(\frac{\partial v_b^g}{\partial t}+\omega\times v_b^g\right)+\sum_{i=1}^{N} m_i r_b^i \times\left[\frac{\partial\omega}{\partial t}\times r_b^i\right]+\sum_{i=1}^{N} m_i r_b^i \times[\omega\times[\omega\times r_b^i]] \tag{11}$$

Eliminating the linear velocity term will give:

$$\sum_{i=1}^{N} m_i r_b^i \times\left[\frac{\partial\omega}{\partial t}\times r_b^i\right]+\sum_{i=1}^{N} m_i r_b^i \times[\omega\times[\omega\times r_b^i]] \tag{12}$$

Simplifying the equation gives:

$$M = I\dot{\omega}+(\omega\times I\omega) \tag{13}$$

Where: $M=[L,M,N]^T$ is the moment, I is the moment of inertia, $\omega=[p,q,r]^T$ is the angular velocity. Rewriting Equation (3) in its respective components:

$$\begin{bmatrix} L \\ M \\ N \end{bmatrix} = \begin{bmatrix} I_{xx} & 0 & I_{xz} \\ 0 & I_{yy} & 0 \\ I_{zx} & 0 & I_{zz} \end{bmatrix}\begin{bmatrix} 1 & 0 & -s\theta \\ 0 & c\phi & c\theta s\phi \\ 0 & -s\phi & c\theta c\phi \end{bmatrix}\begin{bmatrix} \dot{\phi} \\ \dot{\theta} \\ \dot{\psi} \end{bmatrix}+\left(\begin{bmatrix} p \\ q \\ r \end{bmatrix}\times\begin{bmatrix} I_{xx} & 0 & I_{xz} \\ 0 & I_{yy} & 0 \\ I_{zx} & 0 & I_{zz} \end{bmatrix}\begin{bmatrix} p \\ q \\ r \end{bmatrix}\right) \tag{14}$$

Let $\dot{\eta}=[\dot{\phi},\dot{\theta},\dot{\psi}]^T$ and

$$\begin{bmatrix} L \\ M \\ N \end{bmatrix} = \begin{bmatrix} m_{tr}(v_a,h,\delta_{tr}) \\ 0 \\ 0 \end{bmatrix}+\frac{1}{2}\rho v_a^2 s\begin{bmatrix} bC_1(\beta,p,r,\delta_r,\delta_a) \\ cC_M(\alpha,q,\delta_e) \\ bC_n(\beta,p,r,\delta_r,\delta_a) \end{bmatrix} \tag{15}$$

Rewriting the moment equation gives

$$M=\begin{bmatrix} L \\ M \\ N \end{bmatrix} = \begin{bmatrix} m_{tr}(v_a,h,\delta_{tr}) \\ 0 \\ 0 \end{bmatrix}+\bar{q}s\left(\begin{bmatrix} bc_l \\ cc_m \\ bc_n \end{bmatrix}\right)+\begin{bmatrix} bc_{1\delta a} & 0 & 0 \\ 0 & cc_{m\delta e} & 0 \\ 0 & 0 & bc_{m\delta r} \end{bmatrix}\begin{bmatrix} \delta_a \\ \delta_e \\ \delta_r \end{bmatrix}$$

Where $[\delta_a,\delta_e,\delta_r]^T$ are the attitude control inputs $u=[u_1,u_2,u_3]$

Rearranging equation (13) gives

$$I\dot{\omega}=M-(\omega\times I\omega) \tag{17}$$

Substituting in $;\omega=R_2\dot{\eta}$ will give

$$I(\dot{R}_2\dot{\eta}+R_2\ddot{\eta})=M-(R_2\dot{\eta}\times IR_2\dot{\eta}) \tag{18}$$

Finally solving for $\ddot{\eta}$:

$$\ddot{\eta}=(IR_2)^{-1}(-I\dot{R}_2\dot{\eta}-(R_2\dot{\eta}\times IR_2\dot{\eta})+M) \tag{19}$$

Forming a state space, and designing a controller we consider the following assumptions

Let $x_1=\eta$ and $x_2=\dot{\eta}$ hence, $\dot{x}_1=x_2$ and

$$\dot{x}_2=h(x,t)+d(x)u \tag{20}$$

Where

$$h(x,t)=(IR_2)^{-1}(-I\dot{R}_2\dot{\eta}-(R_2\dot{\eta}\times IR_2\dot{\eta})+\bar{q}s[bc_l,cc_m,bc_n]^T)$$

and
$$d(x)=(I\dot{R}_2)^{-1}\begin{bmatrix} bc_{1\delta a} & 0 & 0 \\ 0 & cc_{m\delta e} & 0 \\ 0 & 0 & bc_{m\delta r} \end{bmatrix} \tag{21}$$

Forming the error from the states

$$e=x_d-x_1$$

$h(t,x)=3\dot{x}_9^{\,d}-3x_{10}+\ddot{x}_9^{\,d}-$

2) *Design of NPID Controller for Airspeed Tracking Problem*

The velocity vector that is expressed in wind axes, has an x- component equal to the true airspeed Va and no other components [13]. Hence we will find the airspeed by this method by taking the x component of equation (4) and ignoring the angular rates

$$\dot{v}_a = \dot{u} = \frac{x}{m}$$

$$\dot{v}_a = \frac{1}{m}\left(F_t + \bar{q}\, s c_\alpha c_\beta c_D - mg\right) \qquad (22)$$

Where $g = \begin{bmatrix} -gs\theta \\ gs\phi c\theta \\ gc\phi c\theta \end{bmatrix}$

Since we are going to calculate the x-component we need to express the forces in the wind frame.

$$\dot{v}_a = \frac{c_\alpha c_\beta F_t}{m} + \frac{\bar{q}\, s c_D}{m} - c_\alpha c_\beta s\theta g + s_\beta s\phi c\theta g + s_\alpha c_\beta c\phi c\theta g \qquad \mathbf{(23)}$$

Where Ft= U4.

Forming a state space, and designing a controller we consider the following assumptions

Let $x_3 = v_a$ and $x_4 = \dot{v}_a$ hence $\dot{x}_3 = x_4$ and

$$\dot{x}_4 = h(x,t) + d(x)u \qquad (24)$$

$$h(x,t) = \frac{\bar{q}\, s c_D}{m} - c\alpha c\beta g s\theta + s\beta s\phi c\theta g + s\alpha c\beta c\phi c\theta g \qquad (25)$$

$$d(x) = \frac{c\alpha c\beta}{m} \qquad (26)$$

Forming the error from the states

$$e = x_d - x_3$$

IV. SIMULATION AND RESULT ANALYSIS

A. *Tracking Problem Result*

This section presents the tracking performance of a non-linear PID. The desired value for the attitude and airspeed control has been varied throughout the simulation run time. Initially, the airspeed is thought to be at 12m/s whereas the Euler angles are taken as 0 radians. An external random disturbance is added throughout the simulation time. For phi and psi from -0.7 to 0.7 rad, for theta from -1 to 1 rad and airspeed [230N,350N] at [35s, 60s], this is done to see how much the proposed controller would work in the occurrence of randomness or external disturbance.

Figure 2 shows the NPID controller tracking result for roll control. As seen in figure 2, the actual state of the aircraft can track the reference value. When the desired value changes instantly, the controller can track the change in a short period of time.

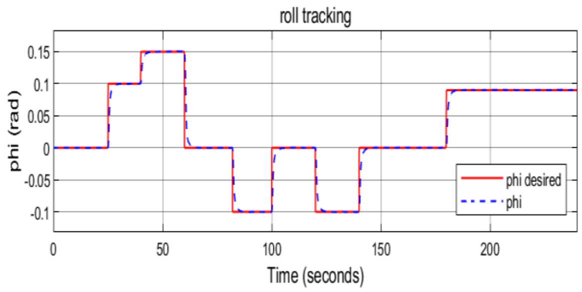

Figure 2. NPID Roll Tracking

Figure 3 shows the NPID controller tracking result for pitch control. As seen in figure 3, the actual state of the aircraft can track the reference value. When the desired value changes instantly, the controller can track the change in a short period of time.

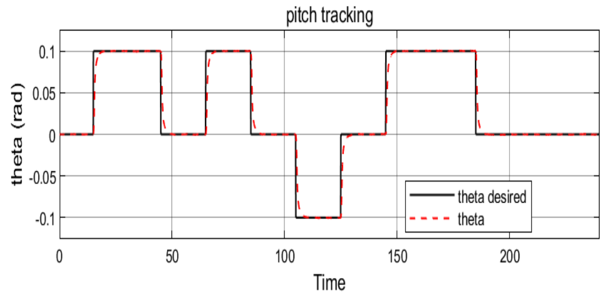

Figure 3. NPID pitch Tracking

Figure 4 shows the NPID controller tracking result for yaw control. As seen in figure 4, the actual state of the aircraft can track the reference value. When the desired value changes instantly, the controller can track the change in a short period of time.

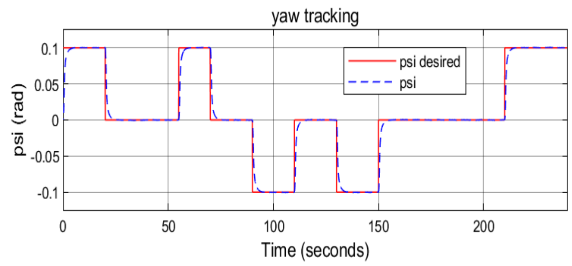

Figure 4. NPID Yaw Tracking

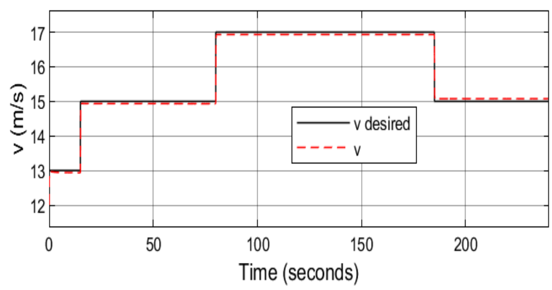

Figure 5. NPID Airspeed Tracking

Figure 5 shows the tracking performance result of the NPID controller for airspeed control. Initially, the state was at 12m/s, and as seen from figure 5 the actual state of the system can track the desired or reference value.

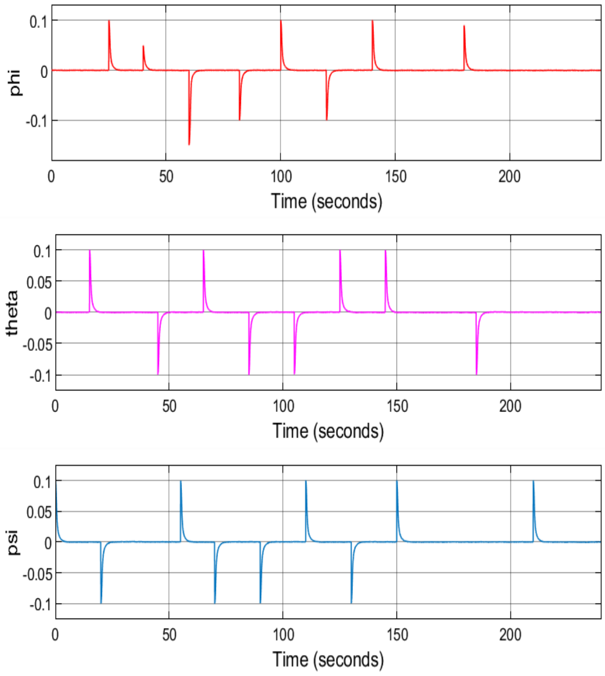

Figure 6. NPID Attitude Error

Figure 6 shows the tracking error of the attitude control phi, theta, psi. As can be seen from figure 6, the error has a spike from -0.1 to 0.1 when there is a change in the desired or reference values. However, it reduces to zero in a very short instant. Furthermore, Figure 7 shows the tracking error for airspeed control. The spikes that occurred when the reference values changes are reduced to zero in a short time.

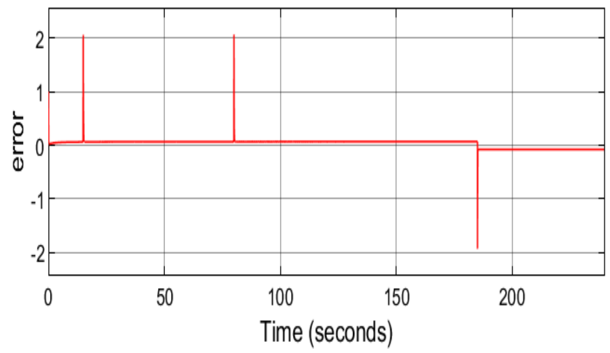

Figure 7. NPID Airspeed Error

B. Input Signal for NPID Tracking Problem

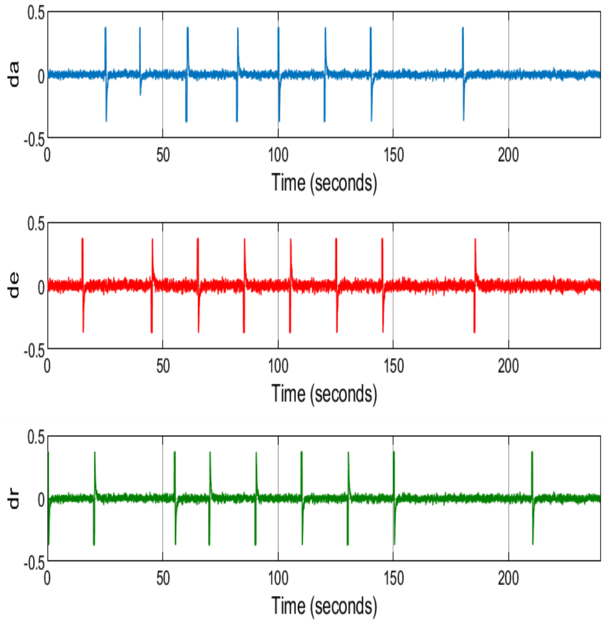

Figure 8. NPID Attitude Control Signal

Figure 8 shows the attitude control inputs whereas Figure 9 shows the control input for airspeed tracking. As seen from figures 8 and 9 the control efforts needed to achieve tracking problems are in an acceptable range. When there is a sudden change in the desired or reference signal, there appears to be a spike in the input signal and that happens because of the controller action that is when the error becomes larger the controller gives more effort (energy) to overcome this change.

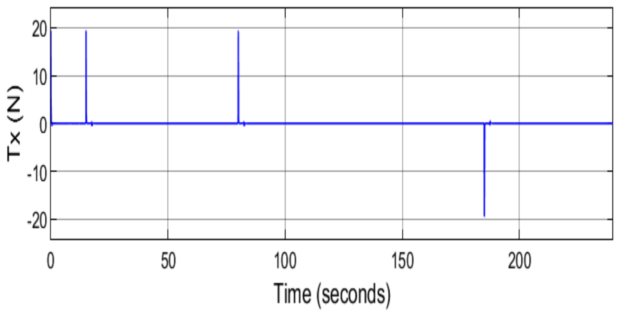

Figure 9. NPID Airspeed Control Signal

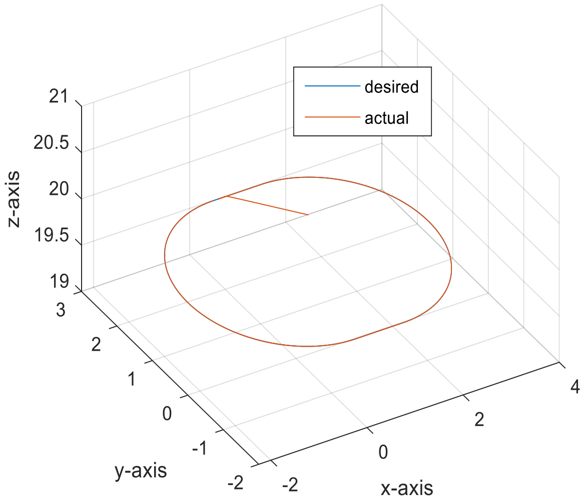

Figure 10. 3D Trajectory Tracking of NPID

Figure 10 shows the three-dimensional trajectory tracking of NPID. From figure 10, it is seen that the states followed the desired trajectory very closely.

TABLE I. FREQUENCY OF NPID TRACKING PROBLEM INPUT SIGNAL

States	Frequency(Hz)
Airspeed	0.7
phi	0.0019
theta	0.0027
psi	0.0019

Table 1 shows the input signal frequency that is given from the system. As seen from table 1, the frequency response of the input signals is good and does not harm devices if implemented in real-time flight.

C. Robustness Analysis

The H2 and H∞ norms are used to check the robustness or the performance of the controller. H2 norm is used to find the energy gain of the system and H∞ is used to find the power gain of the system. This is achieved by taking the norm of the plant's output or the states. Equation (27) and (28) are used to find the H2 and H∞ norms.

$$\|u(t)\|_2 = \sqrt{\int_{-\infty}^{\infty} \sum_i |u_i(\tau)|^2 \, d\tau} \tag{27}$$

$$\|u(t)\|_\infty = \max_\tau(\max_i |u(\tau)|) \tag{28}$$

Consider a system represented as follows

$$\begin{aligned} \dot{x}(t) &= Ax(t) + B_w w(t) + B_u u(t) \\ z(t) &= c_z x(t) + D_{zw} w(t) + D_{zu} u(t) \\ y(t) &= c_y x(t) + D_{yw} w(t) + D_{yu} u(t) \end{aligned} \tag{29}$$

Where x(t) is the state, z(t) is the desired input signal W(t) is the disturbance input. For an impulse input the transfer function G(s) in the frequency domain

$$\lim_{\omega \to \infty} G(j\omega) = 0$$

The controller is robust when the system is strictly casual that is D=0 and the desired input and the measured input are similar because the inputs will depend on the gain value of the states [14]. Analysing H∞ norm to check the robustness of the system, the H∞ should fulfil the following conditions.

$$H_\infty < 1$$

Table 3 shows the H_∞ norm of the system robustness analysis quantitatively. The maximum values for the H_∞ and H_2 is less than one. This indicates that the controller is robust to model uncertainty and external disturbance [15].

TABLE II. NPID ROBUSTNESS ANALYSIS

States	H2	H∞
Airspeed	0.8955	0.99896
phi	0.0003804	2.0854e-4
theta	0.0005432	6.9678e-5
psi	0.0003804	2.085e-4

CONCLUSION

In this paper, modeling and control of a fixed-wing unmanned aircraft is addressed. To find the flight dynamics Newton's second law of motion is used.; a six degree of freedom equation of motion was established and to avoid singularity in the system; the three rotational angles were bounded. To control this non-linear system a non-linear PID control algorithm is designed for tracking problems; for airspeed and attitude control of a fixed-wing unmanned aerial vehicle. To check the robustness of the controllers, an external disturbance is added throughout the simulation time; in addition, the controller gain values are kept in an acceptable range. Furthermore, H2 and H∞ norms have been used to get a numerical representation of the robustness; the frequency of the control signal to the system has been measured. Finally, using the non-linear model of the system; the designed controller is simulated on MATLAB Simulink software. The results show that even when there is an external disturbance, the states followed the desired trajectory. The control signal given to the system has a magnitude that is in an applicable range for equipment. Furthermore, this control signal has a frequency that is not harmful to devices that are used for this system.

FUTURE WORK

For future work, the dynamic modeling of this system can be enhanced by reducing the assumptions taken like the mass being constant. The proposed controller can be further analyzed by hardware in the loop simulation and real-time flight to check their robustness. The tuning mechanism for the non-linear

PID can be extended to other optimal tuning mechanisms.

REFERENCES

[1] M. Albaker and N. A. Rahim, “Flightpath PID controller for propeller-driven fixed-wing unmanned aerial vehicles,” *International Journal of the Physical Sciences 6, no. 8,* pp. 1947-1964, 2011.

[2] Hernandez, J. L, Iván, González-Hernández and RogelioLozano, “Attitude and altitude control for a fixed wing UAV applied to photogrammetry,” *In 2019 International Conference on Unmanned Aircraft Systems (ICUAS),IEEE,* pp. 498-502, 2019.

[3] Arifianto, Ony and M. Farhood, “Optimal control of a small fixed-wing UAV about concatenated trajectories,” *journal of Control Engineering Practice 40,* pp. 113-132, 2015.

[4] T. Espinoza, A. Dzul, L. Rogelio and P. Pavel, “Backstepping-sliding mode controllers applied to a fixed-wing UAV.,” *Journal of Intelligent & Robotic Systems 73,* pp. 67-79, 2014.

[5] Q. Shiyin and S. Amr, “Adaptive PID control of UAV altitude dynamics based on parameter optimization with fuzzy inference,” *International Journal of Modeling and Optimization 6 no. 4,* p. 246, 2016.

[6] Poksawat, Pakorn, W. Liuping and M. Abdulghani, “Gain scheduled attitude control of fixed-wing UAV with automatic controller tuning.,” *IEEE Transactions on Control Systems Technology 26, no. 4,* pp. 1192-1203, 2017.

[7] Ozdemir, Ugur, Mehmet, and K. S, “Linear and nonlinear simulations of aircraft dynamics using body axis system,” *Aircraft Engineering and Aerospace Technology, Istanbul Technical university,* 2008.

[8] B. Niku Saeed, Introduction to robotics: analysis, systems, applications Vol. 7., New Jersey: Prentice hall, 2001.

[9] k. P.Valavanis, Handbook of Unamnned Aerial Vehicles, netherland: springer, 2015.

[10] Su, D. Sun and Duan, “Design of an enhanced nonlinear PID controller,” *Mechatronics 15, no. 8,* pp. 1005-1024, 2005.

[11] Rudd, Ethan, Lalit, Jain, W. J, Scheirer and T. E, “The extreme value machine,” *IEEE transactions on pattern analysis and machine intelligence 40,* vol. 3, pp. 762-768, 2017.

[12] M. Mamo, “Attitude, Heading and Altitude Control of Quadrotor by Designing Higher Order SMC and Non-linear PID Controllers,” *National Repositary of Ethiopia,* msc thesis, 2019.

[13] Randal, Beard W. and Timothy McLain, *Small unmanned aircraft: Theory and practice*, Princeton university press, 2012.

[14] Frazzoli and Emilio, “Dynamic Systems and Control.” *Massachusetts Institute of Technology MIT Open Course Ware* , 2011.

[15] Tijani, Ismaila and B. Agus, “Robust Control using An Extended H∞ Approach: Concepts and Application” *journal of mathematics, statistics and application 1, no. 1, pp. 32-50,* 2016.